Enhanced Spectrum Sharing and Cognitive Radio Using Asynchronous Primary and Secondary Users

Shabnam Sodagari, *Senior Member, IEEE*, and Hamid Jafarkhani, *Fellow, IEEE*

***Abstract*— We show that timing mismatch between the primary and the secondary users results in improving the cognitive radio networks (CRNs) performance. We perform oversampling to exploit the advantages of asynchrony in CRNs. We design detectors for asynchronous transmission to boost the signal received by the primary user in the selfless overlay CRN paradigm. Accordingly, more power is conserved for the secondary user transmission without the performance of the primary user or spectrum license holder being degraded. Simulation results present a green CRN with an almost 6-dB power gain compared with the current CRN frameworks.**

***Index Terms*— Spectrum sharing, cognitive radio.**

I. Introduction

In A selfless overlay cognitive radio network (CRN), the primary user (PU) allows the secondary user (SU) to use its spectral resources, and in return, the SU helps the PU by relaying the PU's message to the PU receiver [1], [2]. Besides, asynchronous communication schemes, in which signals of multiple transmitters arrive with a timing mismatch at the receiver, have been shown to outperform their synchronous counterparts [3], [4]. Nevertheless, to the best of our knowledge, no attention has been paid to taking advantage of the benefits of the timing mismatch between PU and SU in CRNs toward enhancing the performances of these networks via oversampling. The main novelty of this work is that it intentionally adds a timing mismatch between the signals of the PU and SU and designs an appropriate decoder to take advantage of this timing mismatch. This will tremendously improve the performance of a cognitive radio system. The main contributions of this letter address:

1) Improving signal-to-interference-plus-noise ratio (SINR) at the PU and SU receivers by exploiting an intentionally added timing mismatch between the PU and SU;
2) Enhancing the energy efficiency and throughput of the overlay cognitive radio (CR), by proposing an oversampling scheme.

A. Background

Zhai *et al.* [5] investigate an overlay CRN framework, where the SU must learn the PU's message. In this regard, they use linear-assignment Gelfand-Pinsker coding, which requires at least partial channel state information at the transmitter. In addition, Lin *et al.* [6] study a relaying CRN scenario. However, their main goal is to guarantee the PU's secrecy rate, as they consider the SU to be a potential eavesdropper. Lapiccirella *et al.* [7] consider overlay PU and SUs transmissions by allowing the SUs to monitor certain PU control signals in the feedback channel. In their scheme, SUs use a control algorithm to approximate the optimum solution of the SU rate maximization. Nevertheless, in contrast with our method, their method relies on SU having access to PU control channel information. In another study based on overlay CRNs, a distributed opportunistic interference alignment technique that utilizes threshold-based beamforming is used [8]. Their goal is to achieve the full multiplexing gain. Contrary to our work, they assume that the channel state information is available at both the transmitter and the receiver, whereas we assume that this information is only available at the receiver.

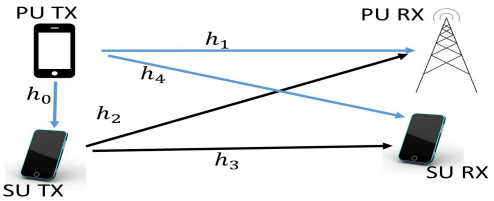

Fig. 1. Cognitive overlay channel with the SU allocating a percent (α) of its power to relay the PU's message x_1 and $1-\alpha$ percent of its power to send the SU's message x_3.

The rest of this letter is organized as follows. In Section II, the structure of the problem and proposed solutions are elaborated. Numerical results that support the effectiveness of the proposed solutions are presented in Section III. Finally, Section IV concludes the letter.

II. System Model and Problem Statement

We consider a cognitive overlay channel with instantaneous power scaling amplify-and-forward relaying as shown in Fig. 1, with TX and RX denoting the transmitter and receiver, respectively. Channel coefficients h_0, h_1, h_2, h_3, and h_4, shown in Fig. 1, are estimated at the receivers. Channel estimation is not specific to our method. Denote PU's message by $x_1(t)$ and the relayed PU's message by the SU as $x_2(t)$. The receiving module of SU TX has noise n_{ST}. We show that the realistic assumption of asynchronous signal reception at the PU and SU receivers leads to a larger SINR. Accordingly, the SU will have to dedicate a smaller portion α of its power to relay the PU's message, without degrading the performance of the PU. Our contribution is to analyze the more realistic case related to time-asynchrony between PU and SU received messages. Fig. 2 shows the sampling scheme [3] deployed at the PU receiver with timing mismatch τ between the PU and SU, which is a fraction of the symbol time T_s. After

Manuscript received October 26, 2017; revised December 16, 2017; accepted December 28, 2017. Date of publication January 9, 2018; date of current version April 7, 2018. This work was supported in part by the NSF Award CCF-1526780. The associate editor coordinating the review of this paper and approving it for publication was O. Amin. *(Corresponding author: Shabnam Sodagari.)*

S. Sodagari is with the Electrical Engineering Department, California State University at Long Beach, Long Beach, CA 90840 USA (e-mail: shabnam@csulb.edu).

H. Jafarkhani is with the Center for Pervasive Communications and Computing, University of California at Irvine, Irvine, CA 92697 USA (e-mail: hamidj@uci.edu).

Digital Object Identifier 10.1109/LCOMM.2018.2789338

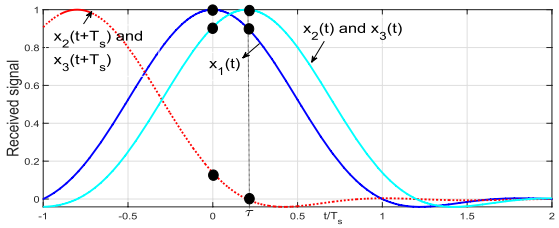

Fig. 2. PU receiver sampling of delayed received signals.

pulse shaping and matched filtering with a raised cosine pulse $p(t) = \text{sinc}(t/T_s)\cos(\pi\beta t/T_s)/\left(1-4\beta^2\, t^2/T_s^2\right)$ [3] (with a roll-off factor β) and inserting $x_2(t) = h_0\sqrt{P_1}x_1(t) + n_{ST}$, we obtain Eq. (1), as shown at the bottom of this page. Here, for the n'th time slot, x_1^n, x_2^n, x_3^n, $n_{ST}^{n,1}$, and $n_{ST}^{n,2}$ are the PU's message, relayed PU's message by the SU, SU's message, and the first and second samples of the Gaussian noise at the receiving module of the SU TX, respectively. $y_P^{n,1}$, $y_P^{n,2}$, $n_p^{n,1}$, and $n_p^{n,2}$ are the first and second samples of PU's received signal, and the first and second samples of PU receiver noise at the n'th time slot, respectively. Also, P_1 and P_2 denote the PU's and SU's transmission powers. In addition, the receivers can utilize blind delay estimation techniques. Similar to channel estimation, the timing estimation can be done for a frame of size N and as long as the frame size is chosen such that during the frame, the changes are not large, the same timing mismatch estimation can be used. Note that $p(T_s-\tau) = 1-p(\tau)$. Also, the raised cosine pulses decay considerably outside of the main lobe. In Eq. (1) we sample the PU received signal twice at every time slot to capture the timing mismatch, as shown in Fig. 2, for N transmitted symbols. To write Eq. (1) in matrix form, for N transmitted symbols, denote the asynchronous signals received by the PU receiver as $\mathbf{Y}^A = [y_P^{1,1}\ y_P^{1,2}\ y_P^{2,1}\ y_P^{2,2}\ \ldots y_P^{n,1} y_P^{n,2}\ \ldots\ y_P^{N,1}\ y_P^{N,2}\ y_P^{N+1,1}]^T$, the vector of desired symbols transmitted from the PU transmitter to the PU receiver as $\mathbf{X}_1 = [x_1^1\ x_1^2\ \ldots\ x_1^n\ \ldots\ x_1^N]^T$, and the noise vector at the

$$
\begin{aligned}
y_P^{1,1} &= \left(h_1\sqrt{P_1} + h_2\sqrt{\alpha P_2 P_1}\,p(\tau)h_0\right)x_1^1 + \underbrace{h_2\sqrt{(1-\alpha)P_2}\,p(\tau)x_3^1}_{\text{CR interference}} + n_p^{1,1} + \sqrt{\alpha}n_{ST}^{1,1}h_2\sqrt{P_2}\\
&\vdots\\
y_P^{n,1} &= \left(h_1\sqrt{P_1} + h_2\sqrt{\alpha P_2 P_1}\,p(\tau)h_0\right)x_1^n + h_2\sqrt{\alpha P_1 P_2}(1-p(\tau))h_0 x_1^{n-1}\\
&\quad + \underbrace{h_2\sqrt{(1-\alpha)P_2}\,p(\tau)x_3^n + h_2\sqrt{(1-\alpha)P_2}(1-p(\tau))x_3^{n-1}}_{\text{CR interference}} + n_p^{n,1} + \sqrt{\alpha}n_{ST}^{n,1}h_2\sqrt{P_2}\\
y_P^{n,2} &= \left(h_1\sqrt{P_1}\,p(\tau) + h_2\sqrt{\alpha P_2 P_1}h_0\right)x_1^n + h_1\sqrt{P_1}(1-p(\tau))x_1^{n+1} + \underbrace{h_2\sqrt{(1-\alpha)P_2}x_3^n}_{\text{CR interference}} + n_p^{n,2} + \sqrt{\alpha P_2}n_{ST}^{n,2}h_2\\
&\vdots\\
y_P^{N,2} &= \left(h_1\sqrt{P_1}\,p(\tau) + h_2\sqrt{\alpha P_2 P_1}h_0\right)x_1^N + \underbrace{h_2\sqrt{(1-\alpha)P_2}x_3^N}_{\text{CR interference}} + n_p^{N,2} + \sqrt{\alpha P_2}n_{ST}^{N,2}h_2\\
y_P^{N+1,1} &= h_2\sqrt{\alpha P_2 P_1}\,p(\tau)h_0 x_1^N + \underbrace{h_2\sqrt{(1-\alpha)P_2}(1-p(\tau))x_3^N}_{\text{CR interference}} + n_p^{N+1,1} + \sqrt{\alpha P_2}n_{ST}^{N+1,1}h_2. \qquad (1)
\end{aligned}
$$

$$
\mathbf{H}_D^A = \begin{pmatrix}
h_1\sqrt{P_1}+h_2h_0\sqrt{\alpha P_1P_2}p(\tau) & 0 & 0 & 0 & \ldots & 0 & 0 & 0 & 0\\
h_1\sqrt{P_1}p(\tau)+h_2h_0\sqrt{\alpha P_1P_2} & h_1\sqrt{P_1}(1-p(\tau)) & 0 & 0 & 0 & \ldots & 0 & 0 & 0\\
\vdots & \vdots & \vdots & \vdots & \vdots & \vdots & \vdots & \vdots & \vdots\\
0 & 0 & \ldots & h_2h_0\sqrt{\alpha P_1P_2}(1-p(\tau)) & h_1\sqrt{P_1}+h_2h_0\sqrt{\alpha P_1P_2}p(\tau) & 0 & 0 & \ldots & 0\\
0 & 0 & \ldots & 0 & h_1\sqrt{P_1}p(\tau)+h_2h_0\sqrt{\alpha P_1P_2} & h_1\sqrt{P_1}(1-p(\tau)) & \ldots & \ldots & 0\\
\vdots & \vdots & \vdots & \vdots & \vdots & \vdots & \vdots & \vdots & \vdots\\
0 & 0 & \ldots & 0 & 0 & 0 & h_2h_0\sqrt{\alpha P_1P_2}(1-p(\tau)) & h_1\sqrt{P_1}+h_2h_0\sqrt{\alpha P_1P_2}p(\tau)\\
0 & 0 & 0 & 0 & \ldots & 0 & 0 & h_1\sqrt{P_1}p(\tau)+h_2h_0\sqrt{\alpha P_1P_2} & \\
0 & 0 & 0 & 0 & \ldots & 0 & 0 & 0 & h_2h_0\sqrt{\alpha P_1P_2}p(\tau)
\end{pmatrix} \qquad (2)
$$

$$
\mathbf{H}_U^A = \begin{pmatrix}
h_2\sqrt{(1-\alpha)P_2}p(\tau) & 0 & 0 & \ldots & 0 & 0\\
h_2\sqrt{(1-\alpha)P_2} & 0 & & 0 & \ldots & 0\\
\vdots & \vdots & \vdots & \vdots & \vdots & \vdots\\
0 & \ldots & h_2\sqrt{(1-\alpha)P_2}(1-p(\tau)) & h_2\sqrt{(1-\alpha)P_2}p(\tau) & \ldots & 0\\
0 & \ldots & 0 & h_2\sqrt{(1-\alpha)P_2} & \ldots & 0\\
\vdots & \vdots & \vdots & \vdots & \vdots & \vdots\\
0 & 0 & 0 & \ldots & 0 & h_2\sqrt{(1-\alpha)P_2}\\
0 & 0 & 0 & \ldots & 0 & h_2\sqrt{(1-\alpha)P_2}(1-p(\tau))
\end{pmatrix} \qquad (3)
$$

PU receiver as $\mathbf{N}^A_{\text{PU}} = [n_p^{1,1}\ n_p^{1,2} n_p^{2,1}, n_p^{2,2}\ \ldots n_p^{n,1}\ n_p^{n,2} \ldots n_p^{N,1}\ n_p^{N,2}\ n_p^{N+1,1}]$. Also, we denote the undesired interference signal at the PU receiver, caused by the message from the SU transmitter intended for the SU receiver, as the vector $\mathbf{X}_3 = [x_3^1\ x_3^2\ \ldots\ x_3^n\ \ldots\ x_3^N]^T$. In the asynchronous case, the signal received by the PU can be written as $\mathbf{Y^A} = \mathbf{H}^A_D\mathbf{X}_1 + \mathbf{H}^A_U\mathbf{X}_3 + \mathbf{N}^A_{\text{PU}}$, where $\mathbf{H}^A_D$ denotes the desired asynchronous channel matrix and $\mathbf{H}^A_U$ denotes the undesired (interference) asynchronous channel matrix, as in Eqs. (2) and (3), as shown at the bottom of the previous page, respectively. Our simulation results and the results of [3] show that compared with the synchronous case, where $\mathbf{Y}^S = \mathbf{H}^S_D\mathbf{X}_1 + \mathbf{H}^S_U\mathbf{X}_3 + \mathbf{N}^S_{\text{PU}}$, in the asynchronous cognitive radio, the matrix $\mathbf{H}^A_D$ results in enhanced detection at the PU receiver. Here, $\mathbf{Y}^S$, $\mathbf{H}^S_D, \mathbf{H}^S_U$, and $\mathbf{N}^S_{\text{PU}}$ are the synchronous counterparts of $\mathbf{Y}^A$, $\mathbf{H}^A_D, \mathbf{H}^A_U$, and $\mathbf{N}^A_{\text{PU}}$, respectively. In other words, $\mathbf{H}^S_D$ is the desired channel, which carries the PU's message from PU and SU transmitters to the PU receiver in the synchronous overlay CRN. In addition, $\mathbf{H}^S_U$ is the undesired (interference) channel between the SU transmitter and PU receiver in the synchronous overlay CRN and $\mathbf{N}^S_{\text{PU}}$ is the noise vector at the PU receiver in the synchronous case. The SINR at the PU RX in the asynchronous case is

$$\gamma_A = \frac{\|\mathbf{H}^A_D\mathbf{X}_1\|^2_F}{\|\mathbf{H}^A_U\mathbf{X}_3\|^2_F + \|\mathbf{N}^A_{\text{PU}}\|^2_F}. \tag{4}$$

The received SINR in the synchronous case is

$$\gamma_S = \frac{\|\mathbf{H}^S_D\mathbf{X}_1\|^2_F}{\|\mathbf{H}^S_U\mathbf{X}_3\|^2_F + \|\mathbf{N}^S_{\text{PU}}\|^2_F}, \tag{5}$$

where $\|.\|^2_F$ denotes the Frobenius norm. For N transmitted symbols, we insert the norms from Eq. (6), at the bottom of this page, into Eqs. (4) and (5) and obtain Eqs. (7) and (8). In Eqs. (6), (7), and (8), σ_s^2 denotes the power of noise at the receiver module of the SU transmitter and σ_p^2 is the noise power at the PU receiver. The main promise of overlay CRN is to provide an acceptable SINR for the PU (by choosing the right α) and use $1-\alpha$ of the power for the SU. We verified through simulations that the PU received SINR in asynchronous overlay CRNs is greater than that in synchronous overlay CRNs. Since time-asynchrony in overlay CRNs results in better SINR at the PU receiver, the constant α can be less than that of synchronous CRNs. As such, $1-\alpha$, which is the amount of power allocated to transmit the SU's message, becomes larger. This shows that more power can be saved for the SU without degrading the PU performance. Oversampling in this case does not require much energy, as the energy-hungry element, i.e., matched filtering, is the same as in the synchronous case. The optimal choice of α can be derived by setting the condition that the PU's SINR is not degraded by the presence of the SU, i.e., $\gamma_A \geq \frac{\|h_1\sqrt{P_1}\|^2}{\sigma_p^2}$. In other words, since the asynchronous cases satisfy the PU's requirements with smaller α, the SU's performance will be improved without degrading the PU's performance.

In addition to the proposed oversampling scheme at the receiver, as shown in Fig. 2, we carry out maximum likelihood sequence estimation (MLSE) using the Viterbi algorithm to avoid the prohibitive complexity of the maximum likelihood (ML) receiver. Viterbi implementation of MLSE is particularly useful when the number of transmitted symbols

$$\begin{aligned}
\|\mathbf{N}^A_{PU}\|^2_F &= (2N+1)\left(\sigma_p^2 + \alpha\sigma_s^2|h_2|^2\ P_2\right)\\
\|\mathbf{N}^S_{PU}\|^2_F &= N\left(\sigma_p^2 + \alpha\sigma_s^2|h_2|^2\ P_2\right)\\
\|\mathbf{H}^A_U\|^2_F &= \|h_2\sqrt{(1-\alpha)P_2}p(\tau)\|^2 + N\|h_2\sqrt{(1-\alpha)P_2}\|^2 + (N-1)\|h_2\sqrt{(1-\alpha)P_2}p(\tau)\\
&\quad + h_2\sqrt{(1-\alpha)P_2}(1-p(\tau))\|^2 + \|h_2\sqrt{(1-\alpha)P_2}(1-p(\tau))\|^2\\
\|\mathbf{H}^S_U\|^2_F &= N\left(|h_2|^2(1-\alpha)P_2\right)\\
\|\mathbf{H}^A_D\|^2_F &= N\|h_1\sqrt{P_1} + h_2h_0\sqrt{\alpha P_1P_2}p(\tau)\|^2 + N\|h_1\sqrt{P_1}p(\tau) + h_0h_2\sqrt{\alpha P_1P_2}\|^2 + \|h_2\ h_0\sqrt{\alpha P_1P_2}p(\tau)\|^2\\
&\quad + (N-1)\|h_2\ h_0\sqrt{\alpha P_1P_2}(1-p(\tau))\|^2 + (N-1)\|h_1\sqrt{P_1}(1-p(\tau))\|^2\\
\|\mathbf{H}^S_D\|^2_F &= N\|h_1\sqrt{P_1} + h_0h_2\sqrt{\alpha P_1P_2}\|^2
\end{aligned} \tag{6}$$

$$\gamma_A = \frac{N\|h_1\sqrt{P_1} + h_2h_1\sqrt{\alpha P_1P_2}p(\tau)\|^2 + N\|h_1\sqrt{P_1}p(\tau) + h_0h_2\sqrt{\alpha P_1P_2}\|^2 + \|h_2\ h_0\sqrt{\alpha P_1P_2}p(\tau)\|^2 + (N-1)\|h_2\ h_0\sqrt{\alpha P_1P_2}(1-p(\tau))\|^2 + (N-1)\|h_1\sqrt{P_1}(1-p(\tau))\|^2}{\|h_2\sqrt{(1-\alpha)P_2}p(\tau)\|^2 + N\|h_2\sqrt{(1-\alpha)P_2}\|^2 + (N-1)\|h_2\sqrt{(1-\alpha)P_2}p(\tau) + h_2\sqrt{(1-\alpha)P_2}(1-p(\tau))\|^2 + \|h_2\sqrt{(1-\alpha)P_2}(1-p(\tau))\|^2 + (2N+1)\left(\sigma_p^2 + \alpha\sigma_s^2|h_2|^2\ P_2\right)} \tag{7}$$

$$\gamma_S = \frac{N\|h_1\sqrt{P_1} + h_0h_2\sqrt{\alpha P_1P_2}\|^2}{N\left(|h_2|^2(1-\alpha)P_2\right) + N\left(\sigma_p^2 + \alpha\sigma_s^2|h_2|^2P_2\right)} \tag{8}$$

$$\begin{aligned}
\begin{bmatrix} y_p^{n,2} \\ y_p^{n+1,1} \end{bmatrix} &= \begin{bmatrix} h_1\sqrt{P_1}p(\tau) + h_2\ h_0\sqrt{\alpha P_2P_1} \\ h_2h_0\sqrt{\alpha P_2P_1}(1-p(\tau)) \end{bmatrix} x_1^n + \begin{bmatrix} h_1\sqrt{P_1}(1-p(\tau)) \\ h_1\sqrt{P_1} + h_2h_0\sqrt{\alpha P_2P_1}p(\tau) \end{bmatrix} x_1^{n+1}\\
&\quad + \underbrace{\begin{bmatrix} h_2\sqrt{(1-\alpha)P_2} \\ h_2\sqrt{(1-\alpha)P_2}(1-p(\tau)) \end{bmatrix} x_3^n + \begin{bmatrix} 0 \\ h_2\sqrt{(1-\alpha)P_2}p(\tau) \end{bmatrix} x_3^{n+1}}_{\text{interference}} + \begin{bmatrix} n_p^{n,2} + \sqrt{\alpha P_2}n_{ST}^{n,2}h_2 \\ n_p^{n+1,1} + \sqrt{\alpha P_2}n_{ST}^{n+1,1}h_2 \end{bmatrix}.
\end{aligned} \tag{9}$$

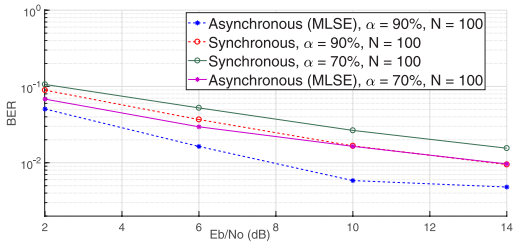

Fig. 3. Comparison of asynchronous and synchronous bit error rates vs. SNR at PU receiver for overlay CRN with $\alpha = 0.7$ and 0.9 for $N = 100$ symbols.

N grows. Asynchronous transmission turns a system without memory into a system with memory. We can deploy this memory at the receiver and use MLSE, whereas the synchronous assumption does not offer this benefit. Note that from Eq. (1) for $2 \leq n \leq N$, we obtain Eq. (9) at the bottom of the previous page. Writing Eq. (9) in matrix form yields $y = \mathbf{P}_n x_1^n + \mathbf{P}_{n+1} x_1^{n+1} + \overbrace{\mathbf{Q}_n x_3^n + \mathbf{Q}_{n+1} x_3^{n+1}}^{\text{interference}} + \mathbf{Z}_{\text{PU}}$. To derive the metric for each path, the likelihood function for Gaussian interference and noise is

$$\mathbb{P}\left(y|x_1^n, x_1^{n+1}\right) = \mathbb{P}\left(\mathbf{d}_n = y - \mathbf{P}_n x_1^n - \mathbf{P}_{n+1} x_1^{n+1}\right) = \frac{1}{\sqrt{2\pi\,|\mathbf{\Sigma}|}} \exp\left(-\frac{1}{2}\mathbf{d}_n^H \mathbf{\Sigma}^{-1} \mathbf{d}_n\right). \quad (10)$$

Here, $\mathbb{P}$ denotes the probability of an event and $\mathbf{\Sigma} = \mathrm{E}[\mathbf{d}_n \mathbf{d}_n^H]$, where E is the expected value. Considering binary phase shift keying (BPSK) modulation, with minimum distance d_{min}, and using the $Q(.)$ function, the probability of error is $\mathbb{P}_e = Q\left(\frac{d_{min}/2}{\sqrt{|\mathbf{\Sigma}|}}\right)$, where $|.|$ denotes the matrix determinant.

III. Simulation Results

Fig. 3 demonstrates the superior bit error rate (BER) performance of our proposed asynchronous transmission and oversampling scheme for overlay CRNs with $\alpha = 0.7$, $\alpha = 0.9$, raised cosine roll-off factor $\beta = 0.6$, $\tau = 0.5\ T_s$, and $N = 100$ transmitted symbols. Simulations were conducted in MATLAB, using BPSK modulation over Rayleigh channels. The receiver uses MLSE Viterbi decoding. As Fig. 3 shows, the asynchronous CRN decreases the BER compared with synchronous cognitive radio. To show the energy efficiency of our proposed oversampling scheme, if we compare, for instance, the BER of a synchronous overlay CRN with $\alpha = 0.9$ at SNR of 14 dB with that of an asynchronous overlay CRN with $\alpha = 0.9$, we observe an almost 6 dB power gain. The SU can use this power gain to reduce α and either save power or allocate a larger portion, i.e., $1-\alpha$ of its power to its own transmission without degrading the received signal at the PU receiver. Fig. 4 with $N = 200$ transmitted symbols and $\alpha = 0.6$, demonstrates the effects of the ratio of transmission powers of PU and SU on the performance of the proposed asynchronous overlay CRN with oversampling at the PU receiver. Our proposed method causes the PU BER to decline faster as the PU power level increases, in comparison with the synchronous case. Fig. 5 (a) shows that the PU BER of asynchronous CRN with $\alpha = 47\%$ is almost equal to the PU BER of synchronous CRN with $\alpha = 60\%$, whereas asynchronous

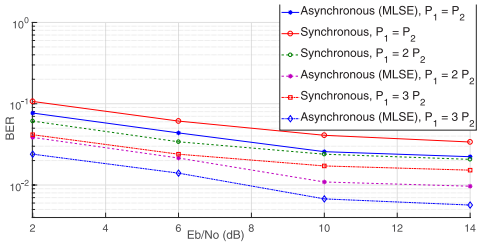

Fig. 4. Bit error rate vs. SNR at PU receiver for various SU and PU power levels.

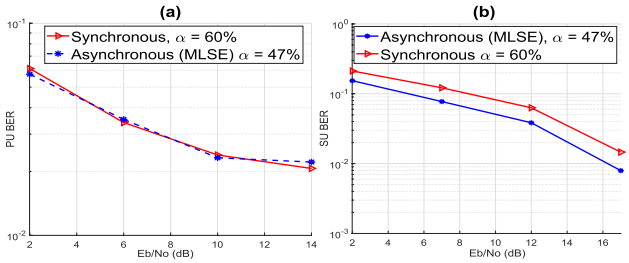

Fig. 5. PU bit error rate (a) and SU bit error rate (b) for asynchronous CRN with $\alpha = 47\%$ and synchronous CRN with $\alpha = 60\%$.

CRN with $\alpha = 47\%$ improves the SU BER compared to synchronous CRN with $\alpha = 60\%$, as shown in Fig. 5 (b).

IV. Conclusions

We took advantage of the real-world phenomenon of asynchronous transmission to improve the performance of cognitive radio networks. We showed that, through receiver oversampling, asynchrony in overlay CRNs results in enhanced SINR at the PU and SU receivers. This reduces the portion α of the SU power dedicated to relaying the PU's message, in exchange for spectrum sharing between the PU and SU. Our proposed asynchronous transmission and oversampling methods allow the SU to save more power for its own message transmission without degrading the PU's performance. The simulation results show an almost 6 dB power gain, which is a promising step toward green cognitive radio and energy efficient spectrum sharing with enhanced throughput.

References

[1] N. Devroye *et al.*, "Cognitive radio networks," *IEEE Signal Process. Mag.*, vol. 25, no. 6, pp. 12–23, Nov. 2008.
[2] E. Biglieri *et al.*, *Principles of Cognitive Radio*. Cambridge, U.K.: Cambridge Univ. Press, Nov. 2012.
[3] M. R. Avendi and H. Jafarkhani, "Differential distributed space-time coding with imperfect synchronization in frequency-selective channels," *IEEE Trans. Wireless Commun.*, vol. 14, no. 4, pp. 1811–1822, Apr. 2015.
[4] S. Poorkasmaei and H. Jafarkhani, "Asynchronous orthogonal differential decoding for multiple access channels," *IEEE Trans. Wireless Commun.*, vol. 14, no. 1, pp. 481–493, Jan. 2015.
[5] J. Zhai *et al.*, "Compress-and-forward based strategy in overlay cognitive radio channel with partial CSIT," in *Proc. IEEE 80th Veh. Technol. Conf. (VTC Fall)*, Sep. 2014, pp. 1–5.
[6] P.-H. Lin *et al.*, "Multi-phase smart relaying and cooperative jamming in secure cognitive radio networks," *IEEE Trans. Cogn. Commun. Netw.*, vol. 2, no. 1, pp. 38–52, Mar. 2016.
[7] F. E. Lapiccirella *et al.*, "Distributed control of multiple cognitive radio overlay for primary queue stability," *IEEE Trans. Wireless Commun.*, vol. 12, no. 1, pp. 112–122, Jan. 2013.
[8] S. Mosleh *et al.*, "Distributed opportunistic interference alignment using threshold-based beamforming in MIMO overlay cognitive radio," *IEEE Trans. Veh. Technol.*, vol. 63, no. 8, pp. 3783–3793, Oct. 2014.